K dependence in the gamma decay of neutron resonances in ^{168}Er and ^{178}Hf

J. Rekstad, T. S. Tveter, M. Guttormsen, and L. Bergholt
Department of Physics, University of Oslo, Norway
(Received 27 July 1992)

The energy-corrected transition rates for γ decay of the n-capture states in ^{168}Er and ^{178}Hf are calculated from data available in the literature. If one assumes that the capture states have good K values, the data reveal a significantly lower average transition rate when the normal K-selection rules are broken than for K-allowed transitions. The effect is more profound in the data from thermal neutron capture than in the data from 2 keV neutron capture.

PACS number(s): 23.20.Lv, 05.45.+b, 21.10.−k, 27.70.+q

I. INTRODUCTION

The projection K of the spin along the symmetry axis of an axially symmetric deformed nucleus plays an important role in the understanding of the structure of low-lying nuclear states. A question of considerable interest is how far up in excitation energy a classification in terms of the K quantum number is useful. Due to the increase in the level density with excitation energy, the Coriolis coupling is expected to cause significant K mixing even for low-spin states, and hence to make a K assignment less adequate.

Furthermore, the nuclear structure reveals signs of chaos [1] at rather low excitation energy. When the nucleus enters the chaotic regime, it is believed that quantum numbers connected with the mean field will lose their significance.

In contrast to this view, theoretical investigations [2] have shown that for a number of nuclei both the axial symmetry and the deformation are surprisingly stable over a considerable energy region. An interesting question is then whether the spin orientation to some extent continues to be influenced by this symmetry.

In a recent letter [3] we investigated the reported intensities [4–7] of the γ transitions following thermal n capture by the two nuclei ^{167}Er and ^{177}Hf, both with a large ground-state K value of $\frac{7}{2}$. Our analysis indicated a K dependence in the γ decay, which we interpreted as a possible result of K hindrance of transitions from the capture states to low-lying levels with K values 0 to 1. According to standard K-selection rules, dipole transitions connecting to these states should be forbidden.

This suggestion has met significant opposition, and alternative explanations have been presented [8,9]. In a recent paper Barrett *et al.* [10] claimed that our results were in conflict with the statistical model. After reexamining the tabulated data of Refs. [4,7], they claimed that our results were not in agreement with the data.

This paper aims to provide the details of our analysis which underlies the conclusion in Ref. [3]. In addition, a similar analysis of reported data [4,7] from 2 keV neutron capture has been performed.

II. METHOD OF ANALYSIS

The capture of neutrons both at thermal energies and at 2 keV is assumed to take place solely through the s-wave channel. The spin of the capture states is then restricted to 3 or 4, with parity equal to the parity of the target ground state.

According to the usual spin coupling scheme, a K value of 3 or 4 can be assigned to the capture states. Also within this scheme the γ-transition rates may be influenced by the K values. One knows from the low-energy regime that a γ transition $K_i \rightarrow K_f$ is K forbidden if $\Delta K = |K_i - K_f| > \lambda$, where λ is the multipolarity of the radiation. The transition rate is then reduced by a factor [11] of approximately $10^{2(\Delta K - \lambda)}$.

This motivates an investigation of the relative γ-ray intensities for transitions from the resonance states to the various low-lying states. All states with spins from 2 to 5 are in principle accessible in direct dipole transitions from the resonance states. Transitions to low-lying states with $K = 0, 1$ are called forbidden, and those to states with $K = 2-5$ are called allowed, in accordance with the standard K-selection rules.

In order to compare the transition rates it is necessary first to correct for the γ-energy dependence. We adopt the energy-corrected intensities given by Refs. [4,5,7], where the intensity is assumed to be proportional to E_γ^5. There might be some dispute about the exponent of 5, but as shown in Ref. [3] the result is not very dependent on an accurate value of this exponent.

The transition probability is also dependent on the spin of the final state. Without detailed knowledge about the structure of both states involved in the transition, this spin dependence is difficult to predict. We therefore determined the average energy-corrected intensity for each spin and parity from the data by

$$\bar{I}(J,\pi) = \frac{1}{N_{J\pi}} \sum_i I_i(J,\pi), \quad I_i(J,\pi) = \frac{I_{\gamma_i}(J,\pi)}{E_{\gamma_i}^5},$$

where the sum is taken over all transitions $I_i(J,\pi)$ in the ensemble. Finally, the energy-corrected intensity of each

individual transition is represented by the ratio

$$x_i = \frac{I_i(J,\pi)}{\bar{I}(J,\pi)} .$$

An eventual K dependence should now be revealed in the distribution of x values obtained for forbidden and allowed transitions, respectively. One may introduce an empirical "hindrance factor" as the ratio $\langle x \rangle_F / \langle x \rangle_A$ of the centroids of the two distributions.

There are evidently a number of error sources in this procedure which should be considered carefully. The limited size, and inhomogeneous composition, of the ensemble we are dealing with may give rise to errors of both random and systematic nature. It should be noted that the variance of the x-value distribution, and, hence, the number of transitions required to achieve a certain degree of statistical confidence, is larger for the thermal than for the average resonance capture (ARC) neutron data set. Thermal neutron capture populates one or two resonances, and the reduced transition rates form a Porter-Thomas distribution, reflecting the microscopic structure of the resonance. This structure dependence disappears due to the statistical averaging over a large number of resonances populated in the ARC experiment.

In order to obtain a sufficiently rich statistical material, the x values deduced from several groups of transitions with different J, π, and K, and even from different nuclei, have to be included. When combining the results from various partial ensembles, variations from subset to subset in the number of allowed relative to the number of forbidden transitions will lead to an incorrect hindrance factor $\langle x \rangle_F / \langle x \rangle_A$. However, it can be shown that errors of this kind in the present case will lower the difference between the two mean values. This issue is discussed in greater detail in Sec. IV.

Even the distinction between forbidden and allowed transitions is not unambiguous. The Coriolis coupling may provide mixing of higher-K components into the wave functions of low-lying states with K quantum number 0 or 1. The importance of this mixing is related to the size of the hindrance factor associated with K-forbidden transitions. This problem will be more thoroughly dealt with in Sec. VIII.

The discussion reveals that the procedure depends on a number of considerations and choices, for instance, concerning the exclusion of certain transitions from the statistics. All such choices, and the sensitivity of the final results upon them, will be accounted for below.

III. ^{168}Er AND ^{178}Hf DECAY SCHEMES

The two nuclei ^{168}Er and ^{178}Hf have been studied extensively, and a large number of rotational bands have been established. Level schemes with the information of importance for the present study are shown in Figs. 1 and 2.

The assignments of the ^{168}Er levels are taken from the work of Davidson and Dixon [12] and references therein. This paper was not available to us during the work with the letter [3], but the assignments are identical to those presented in a previous work by the same authors [6]. Unfortunately, this earlier paper was inadvertently omitted from the list of references in the letter, even though the level scheme underlying our analysis was to a large extent based on this work. We would like to emphasize that this level scheme is more complete than the one employed by Barrett *et al.* [10], which explains the larger number of transitions included in our letter.

To make it easier to compare our work with the results of Barrett *et al.* [10], we have in Sec. IX repeated our analysis using the same level schemes (Refs. [4,7]), as Barrett *et al.* [10]. The level scheme of ^{178}Hf is taken from the work of Hague *et al.* [7].

In ^{168}Er, a total of 46 positive- and 43 negative-parity states have been identified and assigned K values between 0 and 5, as shown in Fig. 1. In ^{178}Hf, 22 positive-parity states and 18 negative-parity states are known. The total ensemble contains 39 states with $K=0,1$ and 90 states with $K=2-5$, among which only four have uncertain K assignments. In the highest excitation region of ^{168}Er the unique assignment of the individual states might be uncertain due to the high level density.

Some of the rotational bands are not complete. There are presumably 11 states missing in the reported level schemes within the considered energy region (shown as dashed levels in Figs. 1 and 2).

The great majority of the reported levels are populated by direct transitions from the capture state. The interpretations and the intensities are based on the results reported in Refs. [4–7,12]. The observed transitions are compiled in Tables I and II for ^{168}Er and ^{178}Hf, respectively. Of the expected 89 transitions in $^{168}\mathrm{Er}_{\mathrm{thermal}}$ only 83 are observed, and 58 out of 61 possible transitions are reported from the $^{168}\mathrm{Er}_{\mathrm{ARC}}$ experiment. This difference in numbers is due to the thermal experiment covering a larger energy interval (up to 2.77 MeV) than the ARC experiment (up to 2.25 MeV). The corresponding numbers for $^{178}\mathrm{Hf}_{\mathrm{thermal}}$ are 38 observed transitions out of 40, and for $^{178}\mathrm{Hf}_{\mathrm{ARC}}$ 35 out of 38.

A substantial number of the transitions appear in multiplets in the γ spectra and their intensities are therefore not directly accessible. These transitions are included in the number of observed transitions given above. In order to extend the statistical material as much as possible, attempts are made to extract intensities from some transitions belonging to doublets. The applied method is described in detail below.

The discrepancy between the number of final states and the number of observed transitions is most likely explained by an intensity of the transitions that is too low. In order to make a correct representation of the intensity distributions, the weak transitions have to be properly treated.

The γ-ray intensities following thermal neutron capture are known to satisfy the Porter-Thomas distribution [13], with a large probability for weak transitions. Missing transitions may have two explanations, provided that the level identification is correct; the transition might be very weak, or the observation may be obscured by transitions from impurities. In Ref. [3] unobserved transitions were included with zero intensity. Due to the opposition by Barrett *et al.* [10], we have adopted a more cautious

and conservative approach. In the present paper the transitions are included only when the γ-ray spectrum is shown and an upper limit of the intensity can be determined. The actual transitions are discussed below.

IV. AVERAGE TRANSITION INTENSITIES

The mean energy-corrected transition intensities for the different spin-parity groups in both nuclei and reactions are compiled in the Tables III and IV.

Due to the small number of transitions in the different groups, the uncertainties in the average values may be large, especially for the thermal neutron data. In order to check this variance, the spin dependence of the average energy-corrected intensities has been investigated for $E1$ and $M1$ transitions and for thermal and ARC data. The results are shown in Fig. 3. The data are presented in a common scale obtained by normalizing the average value for each spin through division by the sum of the centroids for all spins.

It appears from Fig. 3 that there is a similar overall spin dependence for $E1$ and $M1$ transitions, and also for transitions following thermal neutron capture and the capture of 2 keV neutrons. A larger scattering in the mean values from the thermal data than from the ARC data is consistent with the expectations, as pointed out in Sec. II.

The presence of K hindrance makes the average intensities dependent on the ratio between the numbers of allowed and forbidden transitions. If the forbidden transitions on the average are less intense than the allowed transitions, the average intensity determined from a set of individual transitions consisting of many allowed and a few forbidden will be too large. Hence all transitions in the set will be assigned too low x values. However, when this set is added to other sets with a better balance between the number of allowed and forbidden transitions, the many allowed transitions will influence the total ensemble more than a few forbidden transitions. The lack of symmetry in the present data will have the effect that an eventual difference between energy-corrected intensi-

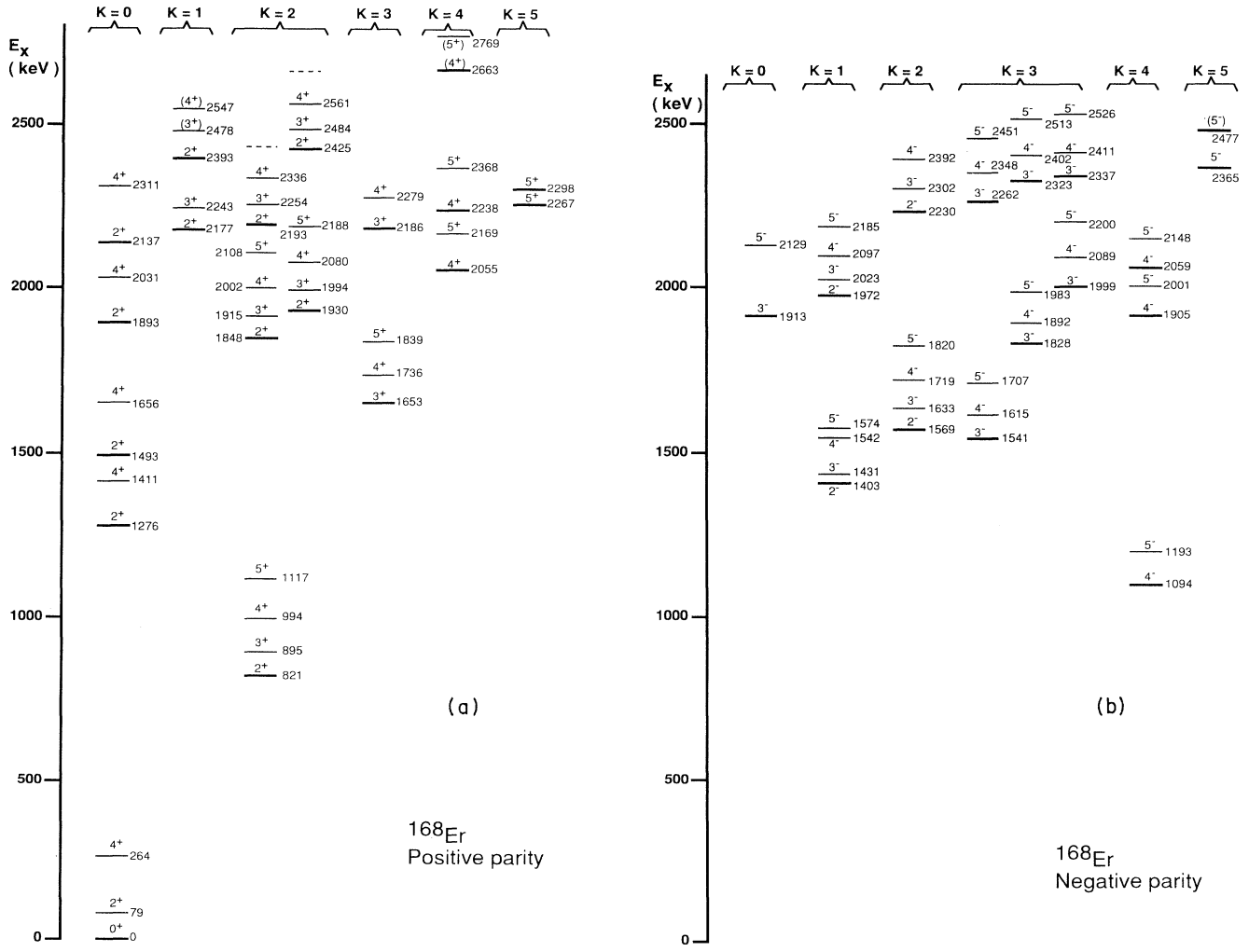

FIG. 1. Partial level scheme of ^{168}Er.

ties for forbidden and allowed transitions will be underestimated.

V. GAMMA-RAY INTENSITIES IN ^{168}Er

A. Gamma rays after thermal neutron capture

The energy-corrected γ-ray intensities after thermal neutron capture are compiled in Table I for transitions to positive-parity states ($M1$) and negative-parity states ($E1$). The x-values are calculated from the average energy-corrected intensities for the respective spin-parity groups given in Table III. In addition to these well established transitions there are a number of multiplets that will be discussed separately.

The transitions are classified according to their final-state K-values. The 33 singlet $E1$ γ transitions comprise 26 allowed and 7 forbidden ones, while the corresponding numbers for $M1$ transitions are 17 and 9.

Two transitions to positive-parity states have been included with intensity zero, one forbidden (2177 keV) and one allowed (2279 keV). Examining the γ spectrum shown in Ref. [4], we observe only vanishing intensities at the expected locations of the γ lines. We have also tentatively assigned zero intensity to a negative-parity state at 2230 keV.

As pointed out above, the thermal data cover a larger energy region than the ARC data. One might have some doubt about the accuracy in the interpretation of the states in this very high excitation region. One should, however, notice that except for one all the transitions into this region are allowed transitions.

A histogram with the number of transitions in each half-digit interval in x is shown in Fig. 4(a).

B. Gamma rays after 2 keV ARC neutron capture

Energy-corrected γ-ray intensities following the capture of 2 keV neutrons are given in Table I. Among the singlet $E1$ transitions there are 17 allowed and 7 forbidden ones. Of the $M1$ transitions 11 are allowed and 8 forbidden.

Within the energy interval studied only two transitions

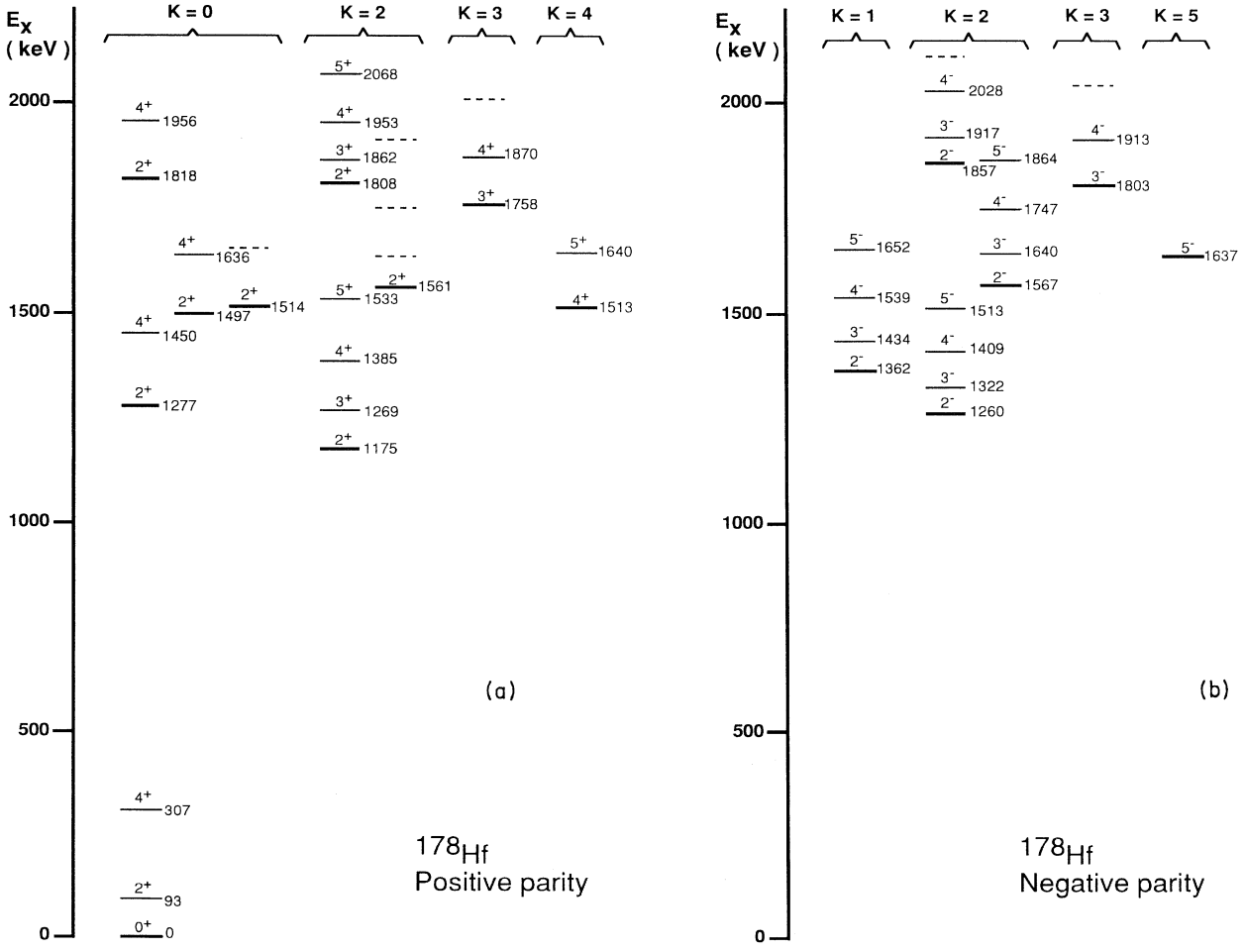

FIG. 2. Partial level scheme of ^{178}Hf.

TABLE I. Primary γ-ray lines from the $^{167}Er(n,\gamma)^{168}Er$ reaction.

Populated state		Thermal n capture[a]		2 keV neutrons[a]	
E_x (keV)	$I^\pi K$	I_γ/E_γ^5	x	I_γ/E_γ^5	x
79	2^+0	1.00	0.26	0.90	1.07
264	4^+0	2.33	0.28	1.83	0.99
821	2^+2	4.50	1.15	0.85	1.01
895	3^+2	1.33	0.16	1.66	0.80
994	4^+2	1.82	0.22	1.56	0.84
1094	4^-4	76.20	1.29	10.34	1.05
1117	5^+2	1.31		1.13	
1193	5^-4	29.32	1.03	4.90	0.98
1276	2^+0	10.80	2.77	0.59	0.70
1403	2^-1	22.90	1.43	5.43	1.36
1411	4^+0	3.31[b]	0.40	1.83	0.99
1431	3^-1	6.16	0.18	8.64	0.97
1493	2^+0	1.25	0.32	1.05	1.24
1541	3^-3	70.32		21.21	
1542	4^-1				
1569	2^-2	18.60	1.16	3.70	0.93
1574	5^-1	24.78	0.87	5.92	1.18
1615	4^-3	3.3[b]	0.06	10.5	1.07
1633	3^-2	73.11	2.10	10.4	1.16
1653	3^+3	8.09	0.96	2.72	1.31
1656	4^+0	4.31	0.52	1.38	0.74
1707	5^-3	25.85	0.91	5.59	1.12
1719	4^-2	61.06	1.04	10.44	1.06
1736	4^+3	11.86	1.43	1.75	0.94
1820	5^-2	27.32	0.96	6.66	1.33
1828	3^-3	30.00	0.86	9.49	1.06
1839	5^+3	5.05		0.74	
1848	2^+2	1.71	0.44	0.3[c]	0.36
1892	4^-3	126.31		11.5	
1893	2^+0				
1905	4^-4	25.81	0.44	9.38	0.96
1913	3^-0	47.10		8.43	
1915	3^+2				
1930	2^+2	3.04	0.78	1.37	1.62
1972	2^-1	6.51	0.41	3.58	0.90
1983	5^-3	15.37	0.54	4.82	0.96
1994	3^+2	7.65	0.91	2.2	1.06
1999	3^-3	58.93	1.70	11.0	1.23
2001	5^-4	15.98		5.7	
2002	4^+2				
2023	3^-1	29.13	0.84	7.79	0.87
2031	4^+0	5.80	0.70	2.21	1.19
2055	4^+4	7.54	0.91	2.37	1.28
2059	4^-4	28.48	0.48	10.15	1.03
2080	4^+2	7.82	0.94	1.92	1.03
2089	4^-3	21.06	0.36	9.59	0.98
2097	4^-1	70.36	1.20	7.49	0.76
2108	5^+2	0[a]		0.96	
2129	5^-0	38.72	1.37	4.12	0.82
2137	$2^+(0)$	0[a]		1.26	
2148	5^-4	33.59	1.19	4.72	0.94
2169	5^+4	3.16		1.28	
2177	2^+1	0[d]	0[e]	0[d]	
2185	5^-1	15.70		7.53	
2186	3^+3				
2188	5^+2				
2193	2^+2	3.65	0.94	0[d]	
2200	5^-3	43.02	1.52	5.00	1.00
2230	2^-2	0[d]		3.27	0.82

TABLE I. (*Continued*).

Populated state		Thermal n capture[a]		2 keV neutrons[a]	
E_x (keV)	$I^\pi K$	I_γ/E_γ^5	x	I_γ/E_γ^5	x
2238	4^+4	16.72	2.01	1.87	1.01
2243	3^+1	4.71	0.56	1.72	0.83
2254	3^+2	5.85	0.70		
2262	3^-3	30.17	0.87		
2267	5^+5	29.01			
2279	4^+3	0[d]	0[e]		
2298	5^+5	6.82			
2302	3^-2	34.91	1.00		
2311	$4^+(0)$	19.49			
2323	3^-3	1.44	0.44		
2336	4^+2	53.08			
2337	3^-3				
2348	4^-3	6.85	0.12		
2365	5^-5	42.82			
2368	5^+4				
2392	4^-2	42.82			
2393	2^+1				
2402	4^-3	73.60	1.25		
2411	4^-3	178.20	3.03		
2425	2^+2	13.41	3.44		
2451	5^-3	20.87	0.74		
2477	(5^-5)	166.06			
2478	(3^+1)				
2484	3^+2	22.61	2.69		
2513	5^-3	51.86	1.83		
2526	5^-3	54.90	1.94		
2547	(4^+1)	0[d]			
2561	4^+2	18.08	2.18		
2663	(4^+4)	9.82			
2769	(5^+4)	65.68			

[a]Intensities without an index are taken from Ref. [4].
[b]The intensities given by Ref. [4] and Ref. [5] are inconsistent. We have taken the lowest value [5].
[c]The intensity is represented by an upper limit. The chosen value is equal to half of this limit.
[d]No intensity reported.
[e]The transition is not listed in Ref. [4], but it appears from the spectrum that it is very weak. The x value has been put equal to zero.

are missing in the ARC experiment. One of these is the transition to the 2177-keV level reported as very weak in the thermal neutron data. The other one feeds the 2193-keV level with $I^\pi K = 2^+2$. Since no spectrum is available in the literature, we have excluded these two transitions from the ARC data set.

The intensity distributions of the γ rays following 2-keV neutron capture are shown in Fig. 5(a).

C. Analysis of doublets

In order to increase the number of states in the ensemble the many doublets have been investigated. The following procedure has been applied.

In general, doublets consisting of states of the same parity have been neglected. The only exception is when the two states have the same spin and both transitions are either allowed or forbidden.

When the doublet is associated with states of opposite parity, the mean energy-corrected intensity of the $M1$ transitions to states of the actual spin is subtracted from the total intensity of the doublet. The difference in intensity is then assigned to the $E1$ transition.

The method is justified by the fact that the $E1$ intensity is on the average five times larger than the $M1$ intensity. This is far more than the variation in $M1$ intensities appearing in the ensemble of transitions. This method is considered to be particularly reliable when applied to the ARC data.

The doublets in the $^{168}\mathrm{Er}_{\mathrm{thermal}}$ spectrum have been analyzed according to this set of rules, and with the following results.

1542 keV.—This peak consists of transitions into the two states $(3^-,3)$ and $(4^-,1)$. The total energy-corrected intensity is 70.3, close to the sum of the average intensities feeding 3^- and 4^- states. One of the transitions belongs to the category "forbidden," while the other is "allowed." We do not see any ways to distribute the intensi-

ty between these transitions.

1892 keV.—This peak corresponds to the final states $(4^-,3)$ and $(2^+,0)$, with a joint energy-corrected intensity of 126.3. The average branching ratio for decay into 4^- versus 2^+ states is 15.3. By subtraction of the average 2^+ intensity from the sum, we obtain an energy-corrected intensity of 122.4 for the transition to the $(4^-,3)$ state.

1914 keV.—The total energy-corrected intensity for $(3^-,0)$ and $(3^+,2)$ is 47.1. The remaining energy-corrected intensity for $(3^-,0)$ is 38.7.

2002 keV.—The total energy-corrected intensity for $(5^-,4)$ and $(4^+,2)$ is 16.0. The remaining energy-corrected intensity for $(5^-,4)$ is 7.7.

2186 keV.—The three states $(5^-,1)$, $(3^+,3)$, and $(5^+,2)$ contribute to this peak. The energy-corrected peak intensity is 15.70. The mean intensity of transitions to 5^- states is 32.7, to 3^+ states 8.4, and to 5^+ states 9.0. The triplet has a total intensity less than half of the average intensities to 5^- states; hence the actual transition has to be weak with x less than 0.5. By subtracting the intensity of the strongest of the two $M1$ transitions, only an intensity of 6.7 is left for the $E1$ transition, corresponding to x less than 0.2. We conclude that the energy-corrected intensity of the transition to the $(5^-,1)$ state is zero.

2337 keV.—The total energy-corrected intensity for

TABLE II. Primary γ-ray lines from the ^{177}Hf$(n,\gamma)^{178}$Hf reaction.

Populated state		Thermal n capture[a]		2 keV neutrons[a]	
E_x (keV)	$I^\pi K$	I_γ/E_γ^5	x	I_γ/E_γ^5	x
93	2^+0	1.00	0.09	54	0.98
307	4^+0	1.92	0.29	100	0.95
1175	2^+2	7.48	0.69	58	1.05
1260	2^-2	2.58		12	0.98
1269	3^+2	25.95		132	
1277	2^+0	5.22	0.48	65	1.18
1322	3^-2	10.02	1.79	16	0.69
1362	2^-1	0[b]		5[b]	0.41
1385	4^+2	6.54	0.99	120	1.14
1409	4^-2	6.68	2.30	19	1.05
1434	3^-1	2.66	0.48	19	0.82
1450	4^+0	4.80	0.73	106	1.01
1497	2^+0	3.43	0.31	33	0.60
1513	5^-2				
1513	4^+4	3.43		168	
1514	2^+0				
1533	5^+2	8.99			
1539	4^-1	0.87	0.30	114	
1561	$2^+(2)$	12.82		45	
1567	2^-2	1.32		20	1.63
1636	4^+0	12.83		122	
1637	5^-5				
1640	3^-2	2.10		64	
1640	5^+4				
1652	5^-1	0.53	0.31[c]	3[b]	0.25
1747	4^-2	0.96	0.33	16	0.88
1758	3^+3	6.20		110	
1803	3^-3	4.03	0.72	20	0.86
1808	2^+2	0.77	0.07	95	1.72
1818	2^+0	45.70	4.19	36	0.65
1857	2^-2	0[b]		0[b]	
1862	3^+2	27.13		150	
1864	5^-2				
1870	4^+3	11.52	1.75	102	0.97
1913	4^-3	16.84		16	0.88
1917	3^-2			38	1.63
1953	4^+2	14.78		105	1.00
1956	4^+0			92	0.87
2028	4^-2	2.94	1.01		
2068	5^+2	1.07			

[a]Intensities taken from Ref. [7].

[b]No intensity reported.

[c]Only one transition to a 5^- state is reported. The x value is determined as explained in the text.

TABLE III. Averaged energy-corrected transition intensities in the ^{168}Er data.

Data	I^π	N_A	N_F	N_{total}	I_γ/E_γ^5
Thermal	2^+	5	4	10	3.93
	3^+	5	1	6	8.37
	4^+	7	4	12	8.26
	2^-	1	2	3	16.0
	3^-	7	3	10	34.7
	4^-	11	1	12	58.9
	5^-	11	2	13	28.3
2 keV	2^+	3	3	6	0.843
	3^+	2	1	4	2.08
	4^+	5	4	9	1.86
	2^-	2	2	4	4.00
	3^-	3	3	6	8.94
	4^-	7	1	8	9.81
	5^-	7	3	10	5.00

TABLE IV. Averaged energy-corrected transition intensities in the ^{178}Hf data.

Data	I^π	N_A	N_F	N_{total}	I_γ/E_γ^5
Thermal	2^+	3	4	7	10.9
	3^+	2	0	2	16.1[a]
	4^+	3	3	6	6.6
	5^+	2	0	2	5.0[a]
	2^-	2	1	3	1.3
	3^-	2	1	3	5.6
	4^-	3	1	4	2.9
	5^-	0	1	1	0.53[b]
2 keV	2^+	2	4	7	55.1
	3^+	3	0	3	126.5[a]
	4^+	2	4	6	105.4
	5^+	2	0	2	68.4[c]
	2^-	2	1	3	12.3
	3^-	3	1	4	23.3
	4^-	3	1	4	18.1
	5^-	0	0	0	12.5[d]

[a]Allowed transitions only.
[b]Forbidden transition only.
[c]Allowed transitions only. The average intensity is based on two transitions appearing in doublets.
[d]No observed transitions. The average intensity is based on the $E1/M1$ ratio for transitions to the other spin states.

TABLE V. Intensities deduced from the analysis of doublets in the ^{168}Er$_{\text{thermal}}$ data.

$I^\pi K$	E_x	I_γ/E_γ^5	x
3^-0	1913	38.7	1.11
5^-1	2185	0	0
4^-2	2392	38.9	0.66
3^-3	2337	44.8	1.29
4^-3	1892	122.4	2.08
5^-4	2001	7.7	0.27
5^-5	2365	33.8	1.19

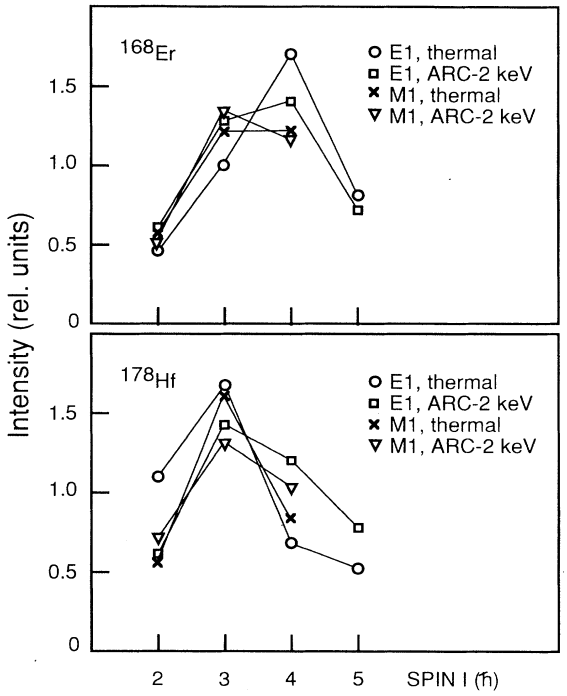

FIG. 3. Average energy-corrected intensities as a function of final spin (for normalization see text).

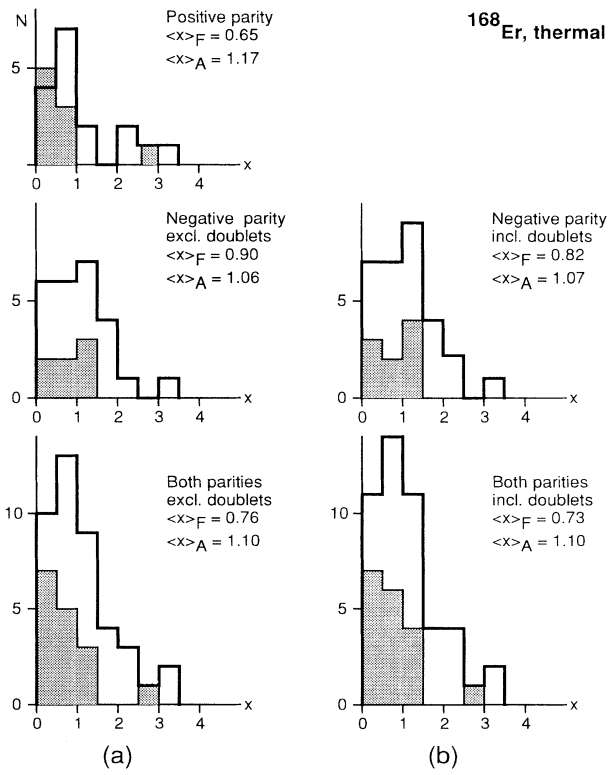

FIG. 4. Number of transitions as a function of relative energy-corrected intensity (x) for ^{168}Er$_{\text{thermal}}$.

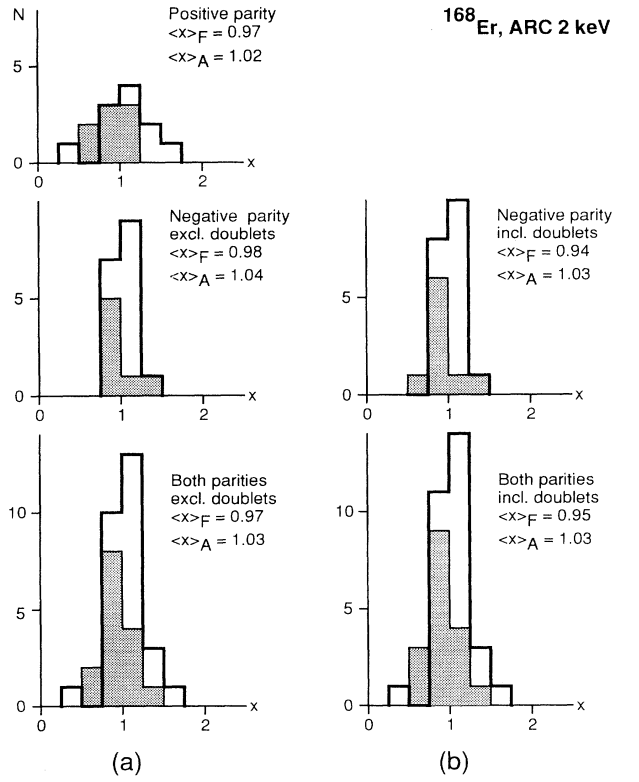

FIG. 5. Number of transitions as a function of relative energy-corrected intensity (x) for $^{168}Er_{ARC\text{-}2\,keV}$.

$(4^+,2)$ and $(3^-,3)$ is 53.1. The remaining energy-corrected intensity for $(3^-,3)$ is 44.8.

2365 keV.—The total energy-corrected intensity for $(5^-,5)$ and $(5^+,4)$ is 42.8. The remaining energy-corrected intensity for $(5^-,5)$ is 33.8.

2392 keV.—The total energy-corrected intensity for $(4^-,2)$ and $(2^+,1)$ is 42.8. The remaining energy-corrected intensity for $(4^-,2)$ is 38.9.

The results for the transitions appearing in doublets in the $^{168}Er_{thermal}$ spectrum are compiled in Table V. These transitions imply only minor modifications in the graphic representation, as seen from Fig. 4(b).

The same procedure has been applied to the doublets in the $^{168}Er_{ARC\text{-}2keV}$ spectrum.

1893 keV.—The total energy-corrected intensity for $(4^-,3)$ and (2^+0) is 11.5. The remaining energy-corrected intensity for $(4^-,3)$ is 10.6.

1914 keV.—The total energy-corrected intensity for $(3^+,2)$ and $(3^-,0)$ is 8.4. The remaining energy-corrected intensity for $(3^-,0)$ is 6.3.

2002 keV.—The total energy-corrected intensity for $(4^+,2)$ and $(5^-,4)$ is 5.8. The remaining energy-corrected intensity for $(5^-,4)$ is 3.9.

2186 keV.—This is the triplet involving the three states $(5^-,1)$, $(3^+,3)$, and $(5^+,2)$. The total intensity of the peak is 7.5. By subtraction of the mean intensities of both of the $M1$ transitions, we get an energy-corrected intensity of 4.4 for the transition to the $(5^-,1)$ state.

The resulting transition intensities are compiled in Table VI. The graph in Fig. 5(b) includes these quantities.

TABLE VI. Intensities deduced from the analysis of doublets in the $^{168}Er_{ARC\text{-}2\,keV}$ data.

$I^\pi K$	E_x	I_γ/E_γ^5	x
3^-0	1913	6.3	0.70
5^-1	2185	4.4	0.88
4^-3	1892	10.6	1.08
5^-4	2001	3.9	0.78

VI. GAMMA-RAY INTENSITIES IN ^{178}Hf

A. Gamma rays after thermal neutron capture

The corresponding results obtained for ^{178}Hf are shown in the Table II. The number of well established and forbidden $E1$ transitions is 6, whereas only 4 allowed transitions, feeding states with spin 2 and 4, are reported. Allowed transitions to spin 3 and 5 are excluded since there are no forbidden transitions to compare the intensities with. Of the reported $M1$ transitions 3 are forbidden and 5 are allowed.

There is only one transition to a 5^- state. In order to determine the x value for the transition feeding the 1652-keV level, we assume that the average energy-corrected intensities for $M1$ transitions show the same spin dependence as the $E1$ transitions, as shown in Fig. 3.

In addition, a 2^- state at 1362 keV is known, but no direct transition from the capture state is reported. Since

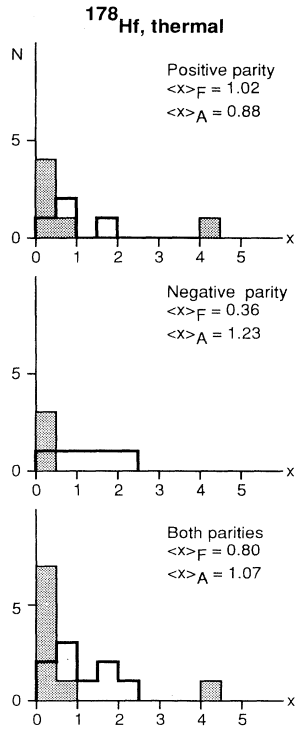

FIG. 6. Number of transitions as a function of relative energy-corrected intensity (x) for $^{178}Hf_{thermal}$.

no spectrum is available, it is not possible for us to estimate an upper limit for the intensity.

A graphic representation of these results is given in Fig. 6.

B. Gamma rays after 2 keV ARC capture

The energy-corrected intensities are given in Table II. The number of well resolved transitions are 11 forbidden and 13 allowed. Among the forbidden transitions 7 are of $E1$ type to spin 2 and 4. The corresponding number of allowed $E1$ transitions is 5. See also the discussion above. The results are presented in Fig. 7(a).

C. Analysis of doublets

The available data do not permit a reliable determination of transition intensities from the doublets reported for $^{178}Hf_{thermal}$.

Since the average energy-corrected intensities are better determined for the ARC data, the doublets in this data set have been investigated. In the following, the same criteria as described in Sec. V C are applied.

1514 keV.—Three transitions contribute to this peak, feeding $(5^-,2)$, $(2^+,0)$, and $(4^+,4)$. The total peak energy-corrected intensity is 168. This is close to the sum of the average values obtained for the spin-parity groups involved, but there is no acceptable method for distribution of the intensity between the transitions.

1535 keV.—The total energy-corrected intensity for $(5^+,2)$ and $(4^-,1)$ is 114. The remaining energy-corrected intensity for $(5^+,2)$ is 96. The transition is not included in the comparison of intensities since the data set does not include any "forbidden" transitions to spin-5^+ states.

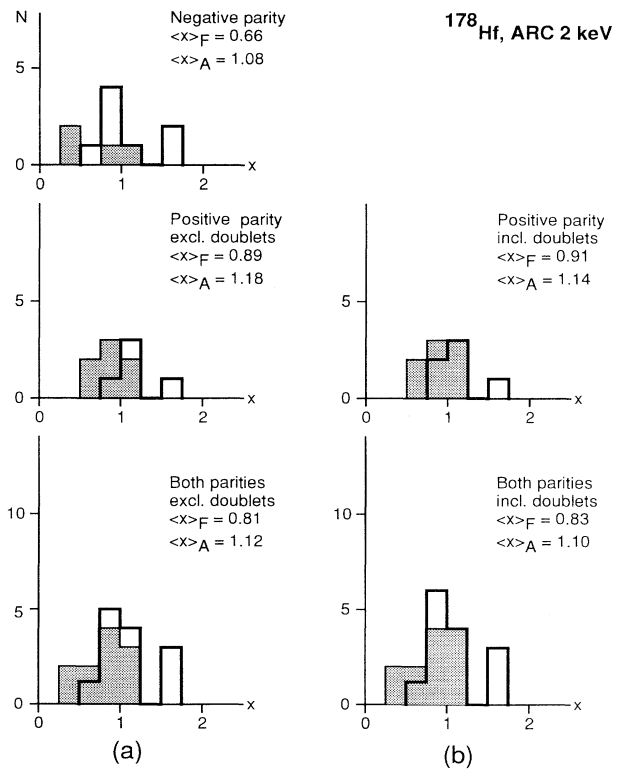

FIG. 7. Number of transitions as a function of relative energy-corrected intensity (x) for $^{178}Hf_{ARC\text{-}2\ keV}$.

TABLE VII. Intensities deduced from the analysis of doublets in the $^{178}Hf_{ARC\text{-}2\ keV}$.

$I^\pi K$	E_x	I_γ/E_γ^5	x
4^+0	1636	110	1.04
5^+2	1533	96	0.91

1636 keV.—Two transitions to $(4^+,0)$ and $(5^-,5)$ states give this peak with a total intensity of 122. The average intensity of transitions to 5^- states cannot be determined directly due to the lack of resolvable transitions. We have estimated the average intensity, from the $E1/M1$ ratio obtained for the transitions to states with lower spins, as 12.5. The subtraction leads to an energy-corrected intensity for the transition to $(4^+,0)$ of 110.

1640 keV.—The total energy-corrected intensity for $(3^-,2)$ and $(5^+,4)$ is 64. The remaining energy-corrected intensity for $(5^+,4)$ is 40.7. Also, this transition is excluded in the comparison of intensities due to the same reason as for the 1535-keV transition.

1862 keV.—The total energy-corrected intensity for $(3^+,2)$ and $(5^-,2)$ is 150. The remaining energy-corrected intensity for $(3^+,2)$ is 137. The transition is not included in the intensity comparison since no "forbidden" transitions to 3^+ states are observed.

The results are summarized in Table VII, and are included in the histogram of Fig. 7(b).

VII. INTENSITIES OF FORBIDDEN AND ALLOWED γ TRANSITIONS

Figures 4–7 reveal a significant difference between the intensity distributions obtained after thermal and ARC neutron capture. In the first case, the intensities are nearly Porter-Thomas distributed, while the ARC data form an approximately Gaussian distribution. Each spectrum contains two distributions, one for the forbidden transitions (hatched) and one for the allowed transitions.

The average x values calculated for the various distributions are listed in the figures. In all cases except one, the forbidden ensembles turn out to have lower centroids than the corresponding allowed ones.

The exception is the distribution of intensities to positive-parity states in ^{178}Hf ($E1$). The six forbidden transitions have $\langle x \rangle_F = 1.02$, while the four allowed transitions have $\langle x \rangle_A = 0.88$. The reason for this untypical result is the one extremely intense transition ($x = 4.19$) to the 2^+0 state at 1818 keV.

The main impression from this analysis is that the forbidden transitions are suppressed compared to the allowed transitions. In the γ decay following thermal neutron capture there is no essential difference between the results obtained for the two nuclei, while the ARC data reveal a much smaller effect in ^{168}Er than in ^{178}Hf.

One should also notice that the inclusion of transitions belonging to doublets does not have an essential effect on the average x values. The present result contradicts a

major point in the criticism raised by Barrett *et al.* [10].

We have added the results obtained for the two nuclei. The distributions are based on 84 and 73 transitions (doublets included) in the thermal and ARC cases, respectively. The ratios between the average x values for forbidden and allowed transitions are 0.69 (thermal) and 0.84 (ARC).

The difference in intensities between forbidden and allowed transitions is much smaller than reported in Ref. [3]. As pointed out above, we have been more restrictive in the selection of transitions this time due to the opposition from Barrett *et al.* [10]. The main reason is, however, that we so far have not taken into account the Coriolis coupling. It is interesting to notice that the suggested effect is visible even before this reduction of the ensemble.

VIII. EXCLUSION OF TRANSITIONS DUE TO CORIOLIS COUPLING

The comparison of forbidden and allowed transition intensities rests on the assumption that the K quantum number of the final states of the transitions is well established. This is indeed not always the case. The main reason for K mixing is the Coriolis force, and this provides a coupling between states of $\Delta K=1$ (first order) and $\Delta K=2$ (second order). The eigenstates will then become a linear combination of different K values.

If the suppression of γ transitions to forbidden states is large, e.g., with a factor $10^{2(\Delta K-\lambda)}$, as in the low-energy regime, even small admixtures of higher K values may strongly influence the transition probability. The applied procedure is then no longer meaningful.

If this hindrance factor for some unknown reason is smaller than in the low-energy regime, the consequence of K mixing will be less dramatic.

It seems in any case well justified to neglect transitions where the final state obviously is Coriolis perturbed. This is only necessary for the forbidden transitions, since minor components of low K values in an allowed state will reduce the transition probability by a small factor only.

In principle one needs an exclusion criterion related to the size of the $K\geq 2$ components mixed into the wave function due to Coriolis coupling. A determination of such components depends on a detailed knowledge of the complete structure, and it is difficult to achieve. A conservative approach is then to exclude transitions to all levels exhibiting significant Coriolis perturbations.

The effect of Coriolis coupling will be evident in the band energies. The perturbation is to the first order revealed in the effective rotational parameter

$$\left[\frac{\hbar^2}{2J}\right]_{\text{eff}}=\frac{E(I_1)-E(I_2)}{I_1(I_1+1)-I_2(I_2+1)} .$$

The level energies in a $K=0$ band are given by the formula [11]

$$E(K,I)=E_K+AI(I+1)+BI^2(I+1)^2+\cdots . \quad (1)$$

For the $K=1$ band one gets an additional term due to matrix elements of the type $\langle K|H_C|\bar{K}\rangle$ which causes a staggering

$$E(I,K)=(-1)^{I+1}I(I+1)[A_2+B_2I(I+1)+\cdots] . \quad (2)$$

The effective rotational parameter for all the apparent $K=0$ and $K=1$ bands in ^{168}Er and ^{178}Hf are shown in Figs. 8 and 9, respectively.

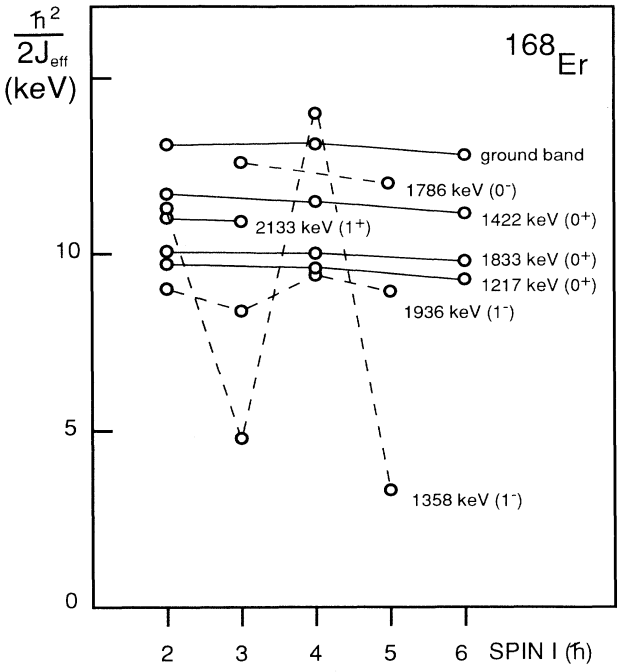

FIG. 8. Effective rotational parameter as a function of spin in ^{168}Er.

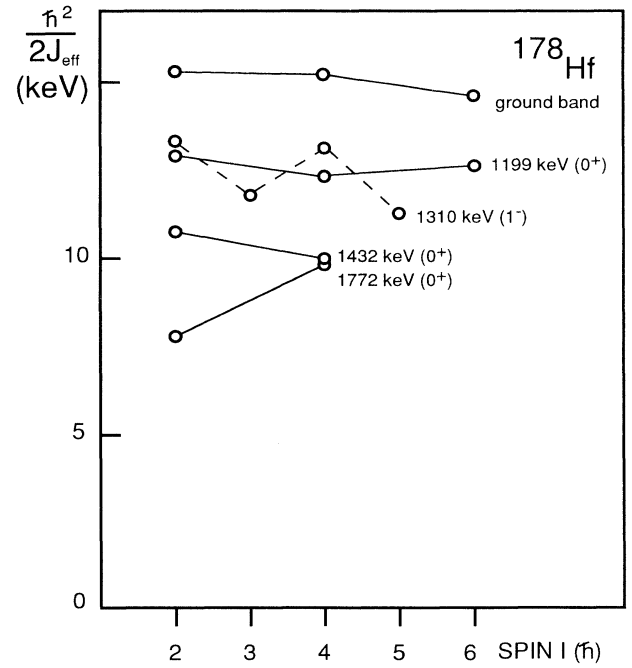

FIG. 9. Effective rotational parameter as a function of spin in ^{178}Hf.

With one exception, the $K=0$ bands show a slightly declining rotational parameter with increasing spin, as expected from Eq. (1). The exception is the 1772-keV (0^+) band in ^{178}Hf, which shows clear signs of strong Coriolis coupling. The rotational parameter is very small, and it increases with increasing spin. Consequently, the most obvious transitions to exclude due to Coriolis coupling are the transitions to the 1818-keV (2^+) and the 1956-keV (4^+) members of this band. One should notice that the forbidden transition to the 1818-keV level was the most intense transition in the total ^{178}Hf ensemble.

Another anomalous $K^\pi=0^+$ band is the 1217-keV band in ^{168}Er. The rotational parameter is much smaller than expected for a band at this excitation energy. Vibrational bands have rotational parameters that are typically a few percent smaller than for the ground band [11]. Due to the blocking effect, rotational bands built on two quasiparticle states may exhibit rotational parameters 30–50 % smaller than for the ground band. From the excitation energy one should expect that the intrinsic state at 1217 keV is due to collective degrees of freedom, but it has been shown [14] that this is not the case. Burke, Maddock, and Davidson [15] determined the structure of this state to be essentially a two quasineutron state $[\frac{7}{2}^+(633)]_{2n}$. This particular structure is expected to be sensitive to rotation due to the large j value and orientation, which might account for parts of the small effective rotational parameter. However, we find these arguments too speculative to justify an exclusion of the transitions to the 1217-keV band from the ensemble.

The staggering expected from Eq. (2) is evident in all the negative-parity $K=1$ bands (dotted lines), and is a measure of the $\Delta K=2$ Coriolis interaction between time-reversed terms in the wave function. This coupling, which splits the band into two signatures, does not change the K composition. Hence, the staggering is not quantitatively related to the content of $K\geq 2$ components in the wave function. A possible admixture of this kind might, however, be traced in the Routhians, shown in Fig. 10. We use the notation given in Ref. [16].

The slope of the Routhian depends on the alignment of spin along the rotational axis. The Coriolis coupling to other bands is normally different for the two signatures, and will give rise to signature splitting. Only the 1358-keV band in ^{168}Er exhibits significant signature splitting for the spins considered here. It is evident that the 2^- and 4^- members of this band correspond to less alignment and thus a larger average K than the 3^- and 5^- members. We have therefore excluded the transitions to 2^- (1403 keV) and 4^- (1542 keV) from the ensemble.

The reduction of the ensemble due to Coriolis perturbation leads to a significant modification of the average energy-corrected transition intensities obtained in thermal neutron capture. The average energy-corrected intensity $\langle x\rangle_F$ is reduced from 0.77 to 0.59 (including doublets) as a result of the removal of the most Coriolis perturbed states. A similar effect of this correction is not obtained in the ARC data, where the average intensities

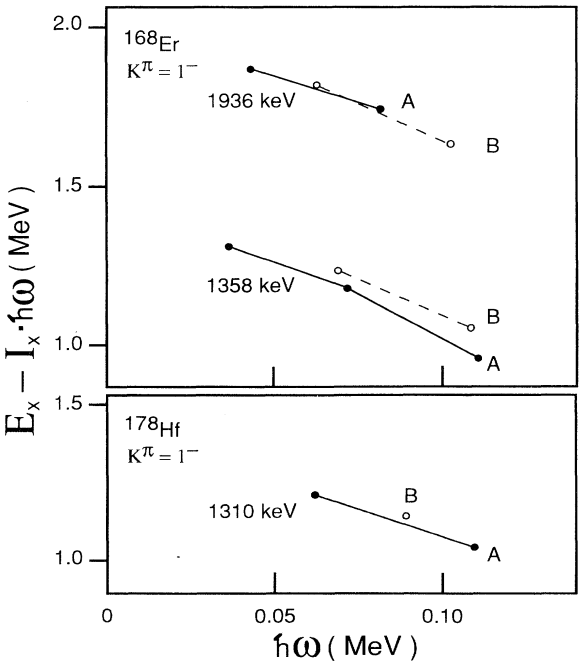

FIG. 10. Experimental Routhians (total) as a function of rotational frequency.

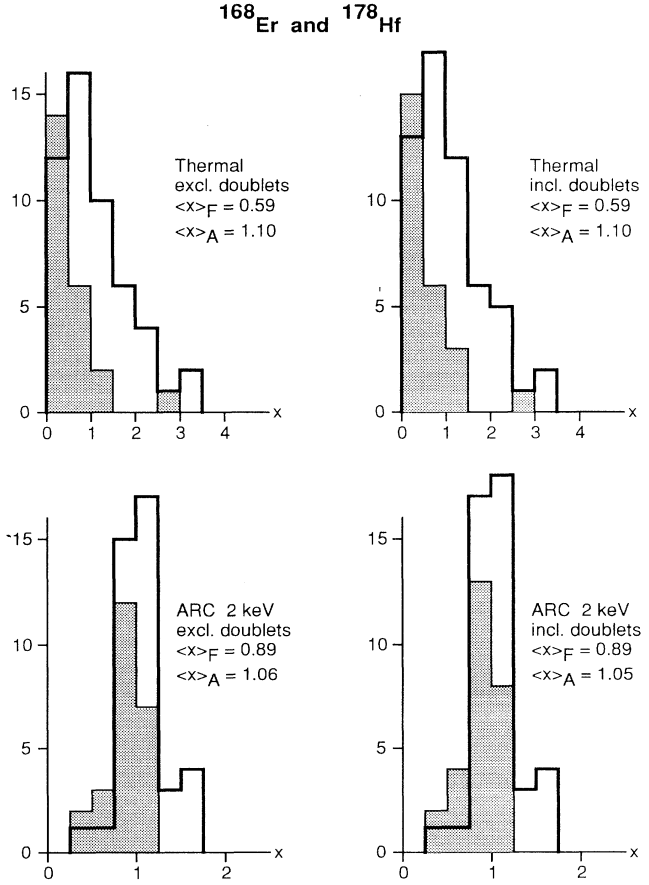

FIG. 11. Number of transitions as a function of x. In his ensemble the most Coriolis perturbed states are excluded (see text).

are nearly unchanged. The resulting intensity distributions are shown in Fig. 11.

IX. COMPARISON WITH THE RESULTS OF BARRETT *et al.*

The thermal neutron capture data reported in Refs. [4,7] have been reexamined by Barrett *et al.* [10], and according to their analysis the ratio of the average intensities of primary γ rays feeding the $K=0,1$ states and the $K=2-5$ states is 0.92. They therefore conclude that there is no significant K dependence in γ decay.

In our analysis we have used the level schemes of Refs. [6,12] and the (n,γ) data of Ref. [5] in addition to the data used by Barrett *et al.* [10]. The extended level scheme of Refs. [6,12] enables us to assign final-state I^{π} values to a larger set of primary γ transitions than allowed by Ref. [4]. To make sure that our results do not depend on whether or not we use this larger data set, we have repeated our analysis using only the transitions reported in Refs. [4,7].

There is a good overall agreement between the relative γ-ray intensities reported in Ref. [4] and Ref. [5], with two exceptions. The transitions to the $4^{+}(0)$ level at $E_x=1411$ keV and to the $4^{-}(3)$ level at $E_x=1615$ keV are both reported in Ref. [4] with intensities approximately ten times larger than those reported in Ref. [5]. It is reasonable in such cases to choose the lowest intensity since there are many ways to observe one specific γ line with a too large intensity (e.g., impurities), while it seems difficult to observe a too low intensity. In spite of this argument we have now excluded these transitions. We have also excluded all unobserved transitions and transitions that occur in doublets.

Without excluding levels due to Coriolis perturbation the ensemble now consists of 23 forbidden and 36 allowed transitions with average energy-corrected intensities $\langle x\rangle_F=0.85$ and $\langle x\rangle_A=1.06$, respectively. This gives a ratio of $\langle x\rangle_F/\langle x\rangle_A=0.79$. After excluding transitions to Coriolis perturbed states according to the method described in Sec. VIII, $\langle x\rangle_F$ reduces to 0.66, and the ratio becomes $\langle x\rangle_F/\langle x\rangle_A=0.62$. This is in agreement with the results which were obtained by us using the more complete level scheme of Refs. [6,12].

Finally, we have repeated our analysis including the transitions to the levels at $E_x=1411$ keV and $E_x=1615$ keV using the high intensities reported in Ref. [4]. The average energy-corrected intensities now become $\langle x\rangle_F=0.92$ and $\langle x\rangle_A=1.02$ before excluding transitions to Coriolis perturbed states. The corresponding ratio is $\langle x\rangle_F/\langle x\rangle_A=0.90$. After excluding transitions due to Coriolis perturbation, $\langle x\rangle_F$ reduces to 0.75, and the ratio becomes $\langle x\rangle_F/\langle x\rangle_A=0.73$.

We have to conclude that even if we only use the data reported in Refs. [4,7], we still get a significantly lower ratio than Barrett *et al.* [10].

X. SUMMARY AND CONCLUSIONS

This detailed discussion of the investigation of γ intensities in ^{168}Er and ^{178}Hf after neutron capture has been carried out as a response to the criticism [10] of a recent letter by three of the present authors (J.R., T.T., and M.G.). As pointed out above the analysis performed is not straightforward; a number of choices have to be made, and some could be criticized. Our approach has been changed accordingly. The present paper is sufficiently detailed to enable the reader to follow the different steps and to judge our interpretations and choices.

We will have to conclude that there is a substantial probability for the resonance states in the nuclei studied, populated by thermal neutrons, to decay by so-called allowed transitions. Barrett *et al.* [10] found a ratio of 0.92 between the intensities for forbidden and allowed transitions. We find this ratio to be 0.69 before corrections for Coriolis coupling, and 0.54 after the exclusions of the most perturbed final states. The corresponding ratio extracted from the decay pattern after 2 keV neutron capture is closer to unity, 0.84, but still statistically significant.

Due to the complexity of the procedure applied, we have made no attempt to calculate the statistical uncertainties of the hindrance factors explicitly. The significance of the effect should be amply demonstrated by the figures.

As revealed by the analysis of Barrett *et al.* [10] the possible effect might have grave implications for our understanding of the nuclear structure near the neutron binding energy. The experimental results available today are probably not conclusive enough to finally settle this question. Of particular importance are those transitions not reported, probably because they are too weak to be seen.

Financial support by NAVF is acknowledged.

[1] H. A. Weidenmüller, in *Proceedings of the Niels Bohr Centennial Conference,* Copenhagen, 1985, edited by R. Broglia, G. Hagemann, and B. Herskind (North-Holland, Amsterdam, 1985), p. 213.

[2] A. L. Goodman, Phys. Rev. C **29**, 1887 (1984).

[3] J. Rekstad, T. S. Tveter, and M. Guttormsen, Phys. Rev. Lett. **65**, 2122 (1990).

[4] W. F. Davidson, D. D. Warner, R. F. Casten, K. Schreckenbach, H. G. Börner, J. Simic, M. Stojanovic, M. Bogdanovic, S. Koicki, W. Gelletly, G. B. Orr, and M. L. Stelts, J. Phys. G **7**, 455 (1981).

[5] W. Michaelis, H. Ottmar, and F. Weller, Nucl. Phys. **A150**, 161 (1970).

[6] W. F. Davidson, W. R. Dixon, and R. S. Storey, Can. J. Phys. **62**, 1538 (1984).

[7] A. M. I. Hague, R. F. Casten, I. Forster, A. Gelberg, R. Rascher, R. Richter, P. von Brentano, G. Berreau, H. G. Börner, S. A. Kerr, K. Schreckenbach, and D. D. Warner,

Nucl. Phys. **A455**, 231 (1986).
[8] T. von Egidy, *Workshop on Nuclear Shapes and Nuclear Structure at Low Excitation Energies,* Cargese, France, 1991 (Plenum, New York, 1993).
[9] P. G. Hansen, Phys. Rev. Lett. **67**, 2235 (1991).
[10] B. R. Barrett, R. F. Casten, J. N. Ginocchio, T. Seligman, and H. A. Weidenmüller, Phys. Rev. **45**, R1417 (1992).
[11] A. Bohr and B. Mottelson, *Nuclear Structure* (Benjamin, New York, 1975), Vol. 2.
[12] W. F. Davidson and W. R. Dixon, J. Phys. G **17**, 1683 (1991).
[13] R. U. Haq, A. Pandey, and O. Bohigas, Phys. Rev. Lett. **48**, 1086 (1982).
[14] A. Bohr and B. R. Mottelson, Phys. Scr. **25**, 28 (1982).
[15] D. G. Burke, B. L. W. Maddock, and W. F. Davidson, Nucl. Phys. **A442**, 424 (1985).
[16] R. Bengtsson and S. Frauendorf, Nucl. Phys. **A327**, 139 (1979).